Journal of Sound and Vibration (1998) **214**(4), 771–778
Article No. sv981635

AN OBSERVATION OF PRESSURE WAVES AROUND A SHALLOW CAVITY

X. ZHANG AND A. RONA
Department of Aeronautics and Astronautics, University of Southampton, Southampton SO17 1BJ, England

AND

J. A. EDWARDS
Weapons Systems Sector, DERA, Fort Halstead, Sevenoaks, Kent TN14 7BP, England

(*Received* 10 *November* 1997, *and in final form* 24 *March* 1998)

A study was performed on supersonic flow over a shallow cavity at Mach 1·5, by using model tests and computational fluid dynamics. Flow visualization techniques including spark schlieren and computational schlieren were employed to identify wave patterns around the cavity and provide insight into major flow physics. The study identified five types of shock/pressure waves around the cavity. In particular, downstream convecting pressure waves associated with large vortices in the driving shear layer were observed. This class of waves has not been reported previously in the open literature. Results suggest that the shear layer is dominated by a coupled motion of flapping in the transverse direction due to the shear layer instability and vortex convection in the streamwise direction due to the non-linear propagation effects leading to significant wave steepening with convection.

1. INTRODUCTION

A shear layer driven turbulent flow in a shallow cavity can develop aerodynamic instabilities which are self-sustained, featuring intense pressure oscillations, vortex shedding, and noise radiation. Recent experimental [1–3] and numerical [4, 5] studies showed a renewed interest in understanding the physics of cavity flow instability, as a basis to develop methods for its suppression [6]. The development/deployment of effective unsteady flow control devices depends on a clear understanding of major flow physics. Despite persistent effort, there are still areas of flow physics and their interpretation which deserve further attention, one of which is the role played by large vortical structures and associated pressure waves in the driving shear layer which are responsible for both narrowband and broadband noise radiation in the far-field. They also determine the characteristics of the shear layer impingement on the downstream face of the cavity. This latter feature is important in that a recent model test [7] has suggested an enhanced oscillation with certain trailing edge geometries.

We wish to contribute to the general debate regarding the flow oscillation mechanism, of which an important feature is the complex wave pattern above the cavity, the observations of which have stimulated past work towards aerodynamic/acoustic feedback models for the self-sustained flow oscillation [8, 9]. Other dominant time-dependent aerodynamic flow features include convectively amplified shear-layer instabilities, convected unsteady vorticity, and unsteady mass entrainment and ejection. These are key factors in generating the complex self-sustained oscillatory flow and are expected to appear

0022–460X/98/290771 + 08 $30.00/0

in aerodynamic models when attempting to address fundamental flow physics. A good review of the subject was given by Neary and Stephanoff [10]. In trying to understand the flow physics, we have employed visualization techniques such as spark schlieren, and computational schlieren.

2. FLOW FIELD AND VISUALIZATION

The particular test case selected in the study is a supersonic flow over a length to depth ratio three cavity at freestream Mach 1·5, with limited discussion of a Mach 2·5 flow. The Reynolds number (Re) based on the cavity depth is $4{\cdot}5 \times 10^5$. A particular feature of the flow is a relatively thick approaching boundary layer. The approaching boundary layer has a thickness of one-third of the cavity depth $D(=15\,\mathrm{mm})$. Experiments including holographic interferometry, spark schlieren and surface pressure were conducted in the

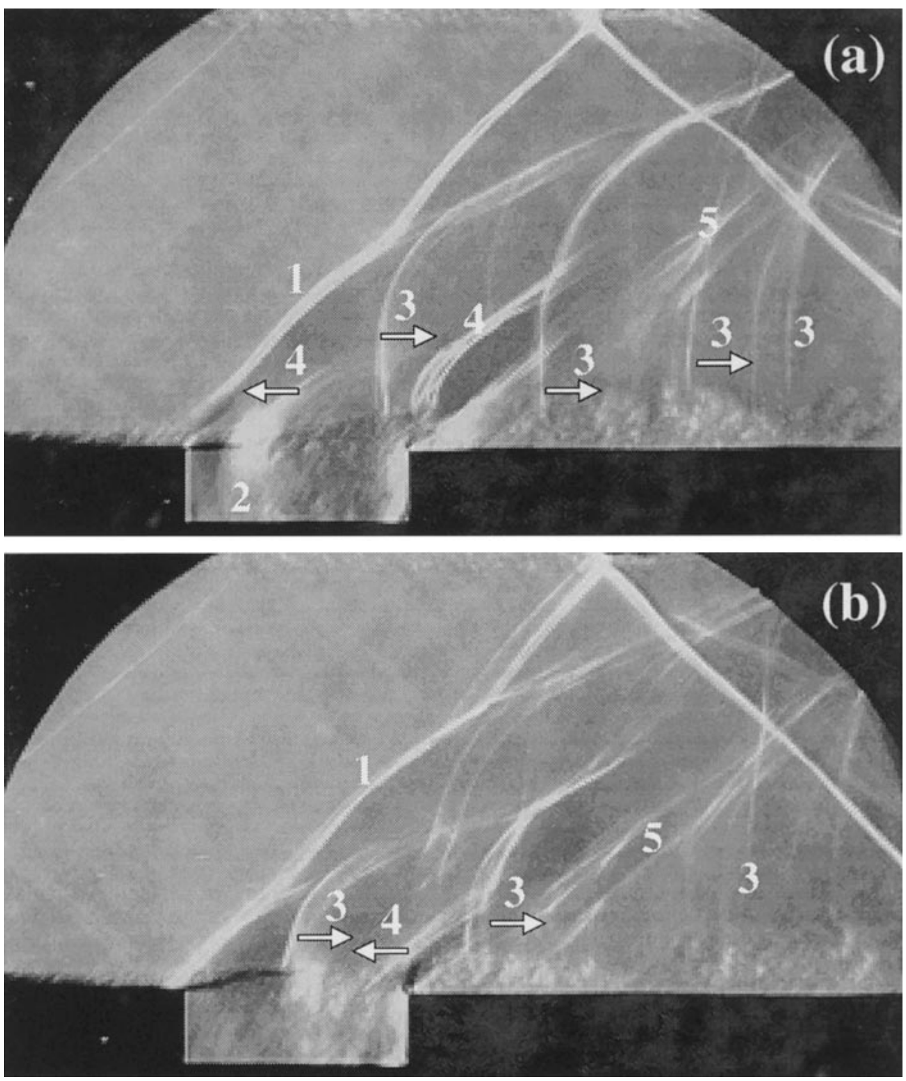

Figure 1. Spark schlieren records of Mach 1·5 flow over a length to depth ratio 3 cavity.

Cambridge University Engineering Department supersonic wind tunnel. The working section is 1219 mm long, 279 mm high and 114 mm wide. A half-liner was used. Details can be found in reference [1].

Numerical models have been developed for the flow which reproduced the large-scale flow features [4, 11]. The phases of the self-sustained instability are captured in the time-dependent predictions, enabling a review of the physical model of the flow. In the current computational schlieren study, we have followed the numerical model developed by Zhang but have increased the accuracy of the time-resolution to second order accuracy. Flow predictions are obtained through solutions of the discrete short-time averaged Navier–Stokes equations with Wilcox's k–ω turbulence model [12]. The numerical algorithms are a development of the method proposed by Zhang, by which time dependent predictions are obtained of the large-scale structure characterizing the unsteady flow. The flow field is discretized by using a multi-block structured grid. A second order Roe flux difference split approximate Reimann solver estimates the inviscid fluxes which are integrated in space with the turbulent fluxes by using a finite volume technique. An explicit multi-step Runge–Kutta scheme with optimized coefficients advances the flow prediction in time. The method is formally second order time and space accurate. The computational domain covers a $12D \times 5D$ area. The domain above the cavity is covered by 320×400 cells and the cavity by 40×40 cells. Details of the model can be found in reference [13].

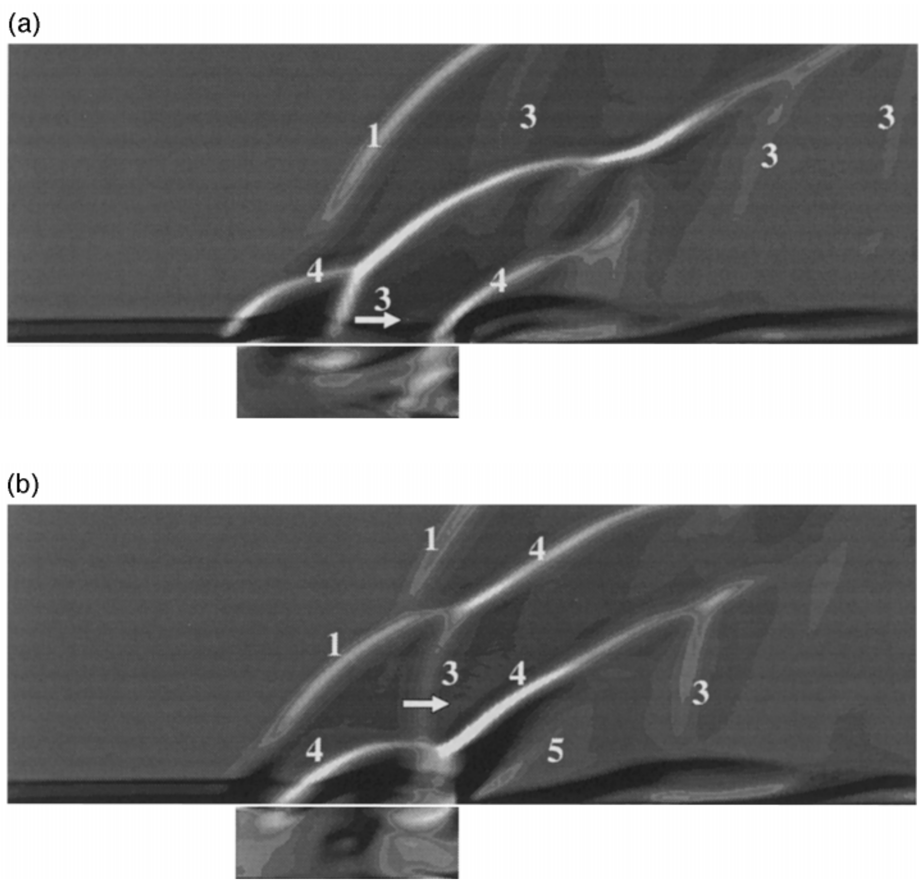

Figure 2(a and b)—(*Caption on following page*).

3. RESULTS AND DISCUSSION

An important feature of the observed flow is the existence of large vortices in the shear layer. The vortices are produced by the shear layer instability which produces flapping motion leading to mass entrainment and ejection at the trailing edge of the cavity. In the current flow, the amplification of the instability waves also leads to non-linear roll-up of the shear layer: i.e., large vortices. The shear layer thus experiences a coupled motion of flapping in the transverse direction and vortex convection in the streamwise direction. The wave pattern above the cavity reflects this mechanism. An example of the wave pattern is shown in the spark schlieren records in Figure 1. The double wave fronts observed in the schlieren records suggest that some three-dimensional effects are present in the model test. However, the flow field can be regarded as basically two-dimensional in nature. The predicted wave patterns are given in Figure 2. In Figure 2, the four computational schlieren images represent a consecutive motion over one oscillation period (T). In the flow, the oncoming turbulent boundary layer is developed on the approaching surface upstream of the cavity. The flow separates at the cavity leading edge as an initially free shear layer, which is unstable under certain flow conditions. Instability modes in the shear flow are convectively amplified, the shear layer displaying vortex roll-up approximately $0{\cdot}5D$ downstream of the leading edge of the cavity. The unsteady velocity and vorticity field

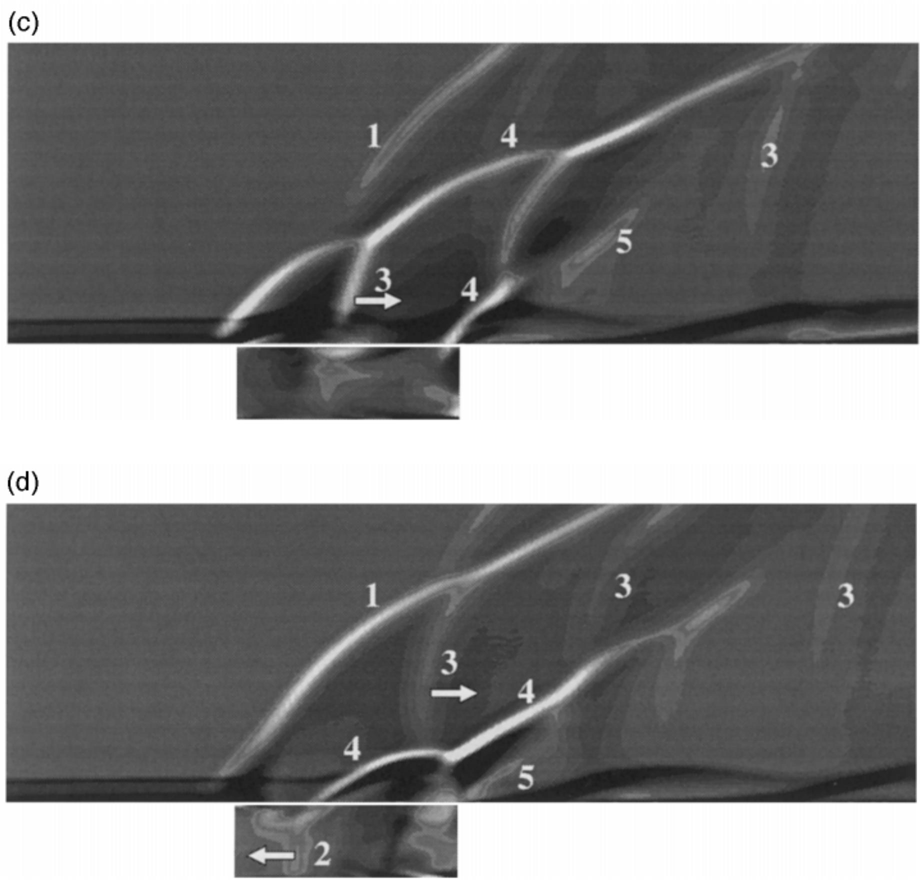

Figure 2. Computational schlieren visualization of flow oscillation over an oscillation period: (a) Time = 0; (b) time = $0{\cdot}25T$; (c) time = $0{\cdot}5T$; (d) time = $0{\cdot}75T$.

interaction with the trailing edge cavity geometry generates an unsteady aerodynamic pressure fluctuation, which propagates upstream as a finite amplitude pressure wave (or disturbances). The wave phase speed is approximately the mean speed of sound in the cavity [3], modified by the unsteady pressure field. Upon reaching the upstream cavity edge, the pressure wave perturbs the shear layer in the vicinity of the edge, closing the feedback loop of the self-sustained cavity flow oscillation.

The instability mode phase speed and cavity length ($3D$) determine the selective amplification of a dominant mode. At Mach 1·5 the measured [1] most amplified mode Strouhal numbers (fD/U_∞) are 0·093, 0·208 (dominant mode), and 0·323. Similar values were obtained in the unsteady computational fluid dynamic predictions [13]: 0·094, 0·194, and 0·369. The agreement between the model test and the numerical prediction is good. The second mode can also be predicted by a modified Rossiter formula given by Heller *et al*. [8], incorporating the effect of temperature difference between the fluid inside the cavity and that in the freestream. The Rossiter/Heller formula gives values of 0·083, 0·194, and 0·305. The 1st and 3rd modes are predicted less well. The semi-empirical formula of Rossiter and Heller, is based on a thin shear layer and was calibrated with the dominant mode of oscillation. It is thus not surprising that only the dominant mode is predicted. When the shear layer is relatively thick as in the present case, modification has to be made with respect to the effect of the thickness of the shear layer on the stability characteristics [1].

The shear layer displacement associated with the convectively amplified velocity/vorticity waves and pressure disturbances in the cavity determines the unsteady wave pattern above the cavity. The observed waves above the cavity can be classified into five types: Type 1 is the leading edge shock-expansion wave caused by the shear layer deflection; Type 2 is the upstream propagating pressure wave inside the cavity; Type 3 is the shock wave associated with the rolling-up of a large vortex in the shear layer and is convected downstream; Type 4 is the shock wave generated by the periodic interaction between the shear layer and the trailing edge. This wave trails the Type 2 wave in the cavity through deflection in the shear layer and moves upstream; In addition there are quasi-stationary waves (Type 5) immediately downstream of the trailing edge (wave-4 of Heller and Delfs [3]). The generation of the Type 1 wave at the leading edge was described by Heller and Delfs [3]. Here our observation suggests that the generation of the wave front is caused by the vortex roll-up and shear layer deflection process. This of course is associated with the pressure disturbances in the cavity. When the shear layer is deflected upwards a shock/compression wave is formed outside the cavity [see Figure 1(b)]. The angle of the wave is determined by the freestream Mach number. When the shear layer is deflected downwards into the cavity and an expansion wave follows the shock/compression wave and the leading edge shock wave is detached from the edge [see Figure 1(a)]; thus the Type 1 wave front exhibits a periodic structure. The length of one particular segment of the periodic wave front gives an indication of the time/frequency of the vortex shedding, upon assuming the length of the segment to be L_1, the freestream Mach number M_∞ and speed U_∞, the frequency of the vortex shedding is given by $L_1\sqrt{M_\infty^2 - 1}/U_\infty$. The Type 2 wave inside the cavity is a weak pressure wave travelling upstream inside the cavity. This weakly compressed wave propagates upstream in the cavity at the local speed of sound. Through the deflected shear layer the external upstream travelling wave (Type 4) trails this wave in the cavity. As the local Mach number outside the cavity is approximately 1·5 and the feedback pressure wave travels at Mach 1·0 in the opposite direction, the angle of the external wave corresponds to approximately the Mach angle at Mach 2·5. Upon reaching the leading edge, the shock detaches from the cavity and moves off into the external stream. The Type 3 wave is directly associated with the

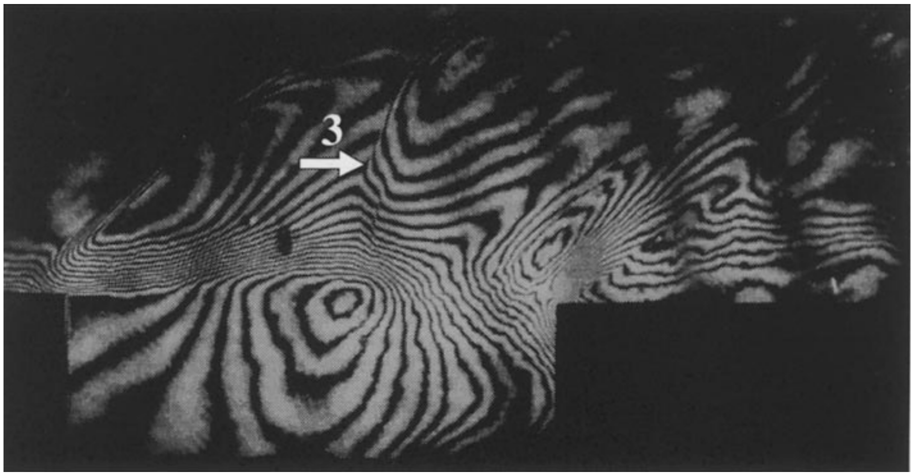

Figure 3. Holographic interferometry record of convecting vortex and Type 3 wave.

forming of the large vortices in the shear layer. The roll-up of the downstream propagating shear layer instability waves inside the shear layer forms the vortices. The vortex shedding is influenced by the modes of the shear layer instability. The continuous shedding of the large vortices creates a downstream travelling wave pattern analogous to the flow past a moving wavy wall. A necessary condition for the forming of the Type 3 wave is $M_e - M_v > 1{\cdot}0$, where M_e is the external flow Mach number immediately outside the shear layer and M_v the equivalent vortex shedding Mach number. This wave is observed in model tests (see Figures 1 and 3). In the model test, the wave angle is measured at $69{\cdot}6^\circ$ in Figure 1(b), indicating an equivalent vortex convection Mach number of 0·43. In the numerical calculation, the Type 3 wave angle at the corresponding position [Figure 2(a)] is given at 68°, suggesting a vortex convecting Mach number of 0·42. Given the uncertainties in the measurement, the agreement is good. To come back to the Type 2 wave, the forming of this wave is closely associated with the shear layer impingement at the trailing edge of the cavity. The impingement process creates a local high pressure and the formation of a strong shock wave near the trailing edge. This is followed by the upstream propagation of a Type 2 wave inside the cavity, which is trailed by a Type 4 wave outside the cavity through the resulting shear layer deflection [see Figure 2(d)]. The movement of the Type 4 wave marks the alternative mass entrainment into and ejection from the cavity trailing edge, following the phases of the dominant instability mode.

In the course of the periodic oscillations, a periodic pattern of wave fronts will appear propagating into the far field. This amounts to noise being radiated from the cavity, in which tones corresponding to the main cavity instability modes characterize the sound pressure level. The peak directivity is expected at the Mach angle to the free stream, where both the upstream propagating waves and the vortex associated convective waves are expected to make contributions. At shallower angles the convected waves alone are expected to contribute to noise.

The coupled motion of the shear layer (flapping in the transverse direction and vortex convection in the streamwise direction) and the associated wave pattern differs from some published results (see, reference [3]). The present study was conducted with a thick approaching boundary layer. The same flow features are also observed at a higher Mach number of 2·5. For the Mach 2·5 flow, the Reynolds number is the same as the Mach 1·5 one and the approaching boundary layer has the same thickness. Both model tests and computational modelling were performed. Since similar results were observed. We will present only an example of the wave front (see the spark schlieren records in Figure 4). A weaker shear layer instability than that at Mach 1·5 is present. In fact, the associated aerodynamic wall pressure fluctuation is lower, the predicted root-mean-square pressure at the downstream edge is $0{\cdot}159\rho_\infty U_\infty^2$ and $0{\cdot}061\rho_\infty U_\infty^2$ at Mach 1·5 and Mach 2·5, respectively. Here, the shear layer instability waves display a moderate convective amplification, without significant non-linear propagation effects observed at Mach 1·5. This prevents any significant wave steepening with convection. Thus only weak Type 3 waves are observed above the cavity open surface [see Figure 4(b)]. The reduction of the aerodynamic unsteadiness at the higher Mach number is predicted by inviscid flow instability theory applied to cavity flow [1]: the wavenumbers of a two-dimensional inviscid unsteady thin shear layer are real above Mach $2\sqrt{2}$; thus the exponentially growing modes at this Mach number could easily be damped.

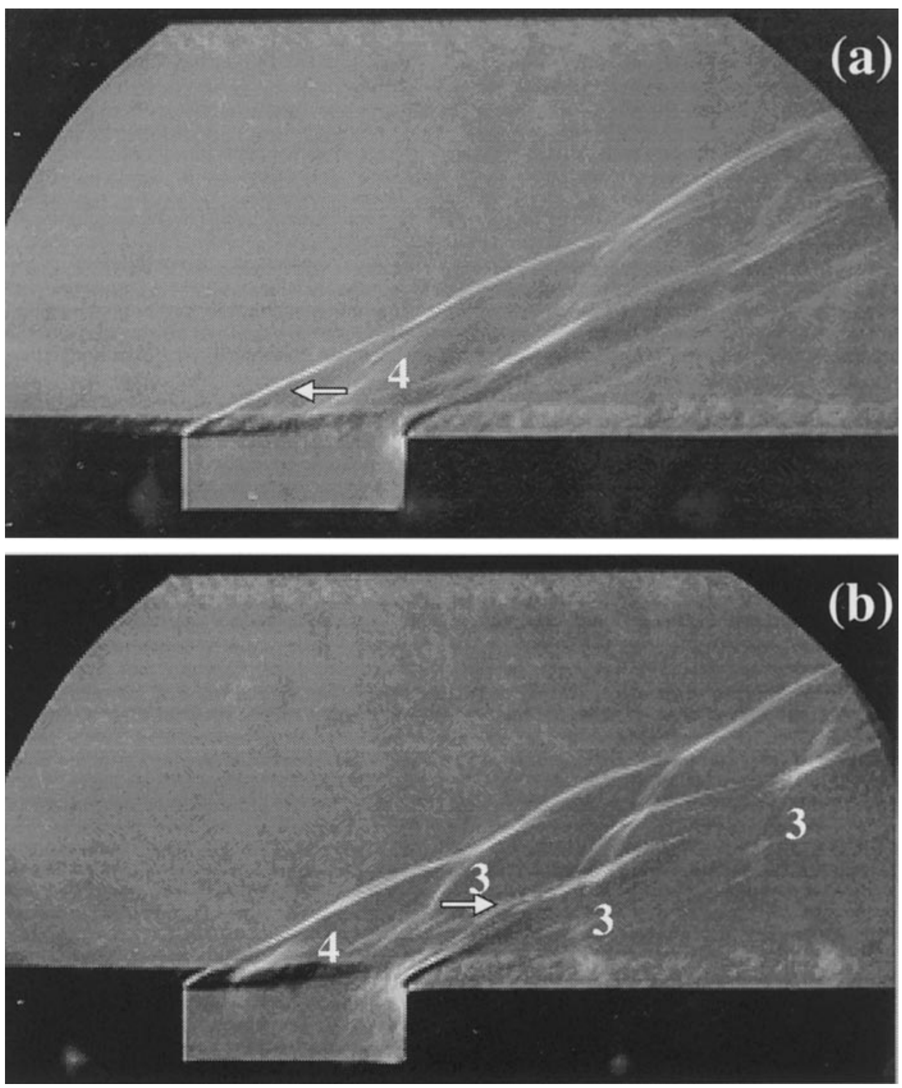

Figure 4. Spark schlieren records of Mach 2·5 flow over a length to depth ratio 3 cavity.

4. SUMMARY REMARKS

Observations have been made of wave patterns above shear layer driven open cavity flows at Mach 1·5. Both model tests and computational modelling were employed with good agreement. The study identifies five types of wave around the cavity. In particular, downstream propagating waves associated with the convecting vortices in the driving shear layer are observed. Results suggest that the shear layer is dominated by a coupled motion of flapping in the transverse direction due to the shear layer instability and vortex convection in the streamwise direction due to the non-linear propagation effects leading to significant wave steepening with convection.

ACKNOWLEDGMENT

The authors thank G. M. Lilley for helpful discussions in preparing the paper.

REFERENCES

1. X. Zhang and J. A. Edwards 1990 *Aeronautical Journal* **94**(940), 355–364. An investigation of supersonic oscillatory cavity flow driven by thick shear layers.
2. K. K. Ahuja and J. Mendoza 1995 *NASA CR*-4653. Effects of cavity dimensions, boundary layer, and temperature on cavity noise with emphasis on benchmark data to validate computational aeroacoustics.
3. H. Heller and J. Delfs 1996 *Journal of Sound and Vibration* **196**(2), 248–252. Cavity pressure oscillations: The generating mechanism visualized.
4. Y. N. Jeng and U. J. Payne 1995 *Journal of Aircraft* **32**(2), 363–369. Numerical study of a supersonic open cavity flow and pressure oscillation control.
5. C. J. Tam, P. D. Orkwis and P. J. Disimile 1996 *AIAA Journal* **34**(11), 2255–2260. Algebraic turbulent model simulations of supersonic open-cavity flow physics.
6. S. McGrath and L. Shaw 1996 *AIAA Paper* 96-1949. Active control of shallow cavity acoustic resonance.
7. J. C. F. Pereira and J. M. Sousa 1994 *AIAA Journal* **32**(8), 1737–1740. Influence of impingement edge geometry on cavity flow oscillation.
8. H. Heller, D. G. Holmes and E. E. Covert 1971 *Journal of Sound and Vibration* **18**(4), 545–553. Flow-induced pressure oscillations in shallow cavities.
9. W. L. Hankey and J. S. Shang 1980 *AIAA Journal* **18**(8), 892–898. Analyses of pressure oscillations in an open cavity.
10. M. D. Neary and K. D. Stephanoff 1987 *Physics of Fluids* **30**(20), 2936–3946. Shear-layer-driven transition in a rectangular cavity.
11. X. Zhang 1995 *AIAA Journal* **33**(8), 1404–1411. Compressible cavity flow oscillation due to shear layer instabilities and pressure feedback.
12. D. C. Wilcox 1988 *AIAA Journal* **26**(11), 1299–1310. Reassessment of the scale determining equation for advanced turbulence models.
13. A. Rona 1997 *Ph.D. Thesis*, *Department of Aeronautics and Astronautics*, *University of Southampton*, *England*. Aerodynamic and aeroacoustic estimations of oscillatory supersonic flows.